

Designing the Folding Mechanics of Coiled Coils

Thomas Bornschlöggl,* J. Christof M. Gebhardt, and Matthias Rief^[a]

Dedicated to Erich Sackmann on the occasion of his 75th birthday

Naturally occurring coiled coils are often not homogeneous throughout their entire structure but rather interrupted by sequence discontinuities and non-coiled-coil-forming subsegments. We apply atomic force microscopy to locally probe the mechanical folding/unfolding process of a well-understood model coiled coil when unstructured subsegments with different sizes are added. We find that the refolding force decreases from 7.8 pN with increasing size of the added unstructured subsegment, while the unfolding properties of the model

coiled coil remain unchanged. We show that this behavior results from the increased size of the nucleation seed which has to form before further coiled-coil folding can proceed. Since the nucleation seed size is linked to the width of the energetic folding barrier, we are able to directly measure the dependence of folding forces on the barrier width. Our results allow the design of coiled coils with designated refolding forces by simply adjusting the nucleation seed size.

Introduction

The coiled coil is a widespread structural motif^[1–3] which often occurs in proteins that are subject to mechanical stress. Examples are actin-binding proteins such as cortexillin (which influences the bending moduli of the plasma membrane),^[4] intermediate filaments, presumably acting as mechanical stress absorbers,^[5] fibrinogen (which is involved in the clotting of blood),^[6] and proteins associated with the fusion of membranes such as the SNARE complexes^[7] or the HIV-gp41 complex.^[8] The structurally simplest coiled coils are double-stranded, which means that they consist of two alpha-helices that wrap around each other. Coiled-coil formation can be predicted from the amino-acid sequence by parametric programs, thus allowing the estimation that between 3 and 5% of all the amino acids occurring in proteins known so far are part of coiled-coil structures.^[1,9] These programs also indicate that often naturally occurring, longer coiled coils are not homogeneous throughout their structure but rather frequently interrupted by non-coiled-coil-forming subsegments. Examples of such non-homogenous coiled coils are the dimerization motifs of dimeric molecular motors of the myosin and kinesin family,^[10,11] the coiled coils composing intermediate filaments^[5] and the extremely long coiled coil in the nuclear mitotic apparatus protein.^[12] Although much effort has been made to understand the folding process of coiled coils, little is known about the local influence of coiled-coil-interrupting subsegments on the folding process.^[13]

An example of a well-studied model coiled coil is the leucine zipper from the yeast transcriptional activator GCN4.^[14] This coiled coil exhibits a nearly perfect heptad repeat, which is only interrupted by a single hydrophilic asparagine (green in Figure 1) within the hydrophobic core of the coiled coil. The two-state folding mechanism of this coiled coil, with a covalent cross-link at the C-terminal end is outlined in Figure 1.

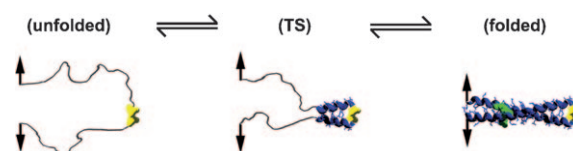


Figure 1. Schematics of the two-state folding process of the LZ10 model coiled coil, which is covalently connected at the C-terminus via a disulfide bridge (yellow atoms). 14 C-terminal amino acids of every strand have to contract against the N-terminal-applied force in order to build a nucleation seed corresponding to four alpha-helical turns per strand. After formation of the nucleation seed (TS), coiled-coil folding occurs in a down-hill-like fashion.

Due to the introduction of a covalent cross-link, folding starts robustly at the cross-linked end^[15] via the formation of a nucleation seed. This seed formation involves the C-terminal collision of the two unstructured or only sparsely alpha-helically structured coiled-coil chains, which leads to a C-terminal coiled-coil part consisting of four alpha-helical turns.^[15–18]

After formation of the nucleation seed [transition state (TS) in Figure 1], the rest of the coiled-coil zipping occurs in a down-hill-like manner. We have recently shown that atomic force microscopy (AFM) is ideally suited to locally measure the mechanical folding process of single coiled coils and to determine the size of the nucleation seed directly without the use of mutations.^[19,20] Using this technique, we have confirmed that the nucleation seed of a model coiled coil (LZ10) which is closely related to the GCN4 zipper, consists of four alpha-helical turns at the C-terminal end. Moreover we could show that formation of this nucleation seed occurs against an applied force of 7.8 pN.^[19,20]

[a] Dr. T. Bornschlöggl, J. C. M. Gebhardt, Prof. Dr. M. Rief
Physik Department E22, Technische Universität München
James Franck Strasse, 85748 Garching (Germany)
Fax: (+49) 89-289-12523
E-mail: mrief@ph.tum.de

Results and Discussion

Herein, we apply AFM to locally probe the effect of the C-terminal addition of unstructured subsegments with different lengths on the mechanical folding mechanism of the LZ10 coiled coil. We added 10 and 20 amino acids, respectively to the C-terminal end of the LZ10 coiled coil leading to the constructs LZ10₊₁₀ and LZ10₊₂₀. The total amino-acid sequences of the resulting constructs are given in the Experimental Section. The inserted amino-acid sequences were taken from the hinge region of the *Drosophila melanogaster* kinesin coiled coil, because it is well-known that this sequence does not form any secondary structures—even within a coiled-coil environment.^[22–25] The expected schematic structures of the constructed proteins are shown in Figure 2d).

Figures 2a–c show the averaged unzipping (black) and reziping (blue) force extension traces of the constructed coiled coils. The experimental setup and the averaging technique are explained in the Experimental Section. In brief, globular protein domains are added to the N-terminal end of the coiled coil, thereby acting as handles to which the AFM cantilever tip and

the substrate of the AFM can bind. By measuring and averaging about 60 single unzipping and reziping force-extension traces of the respective coiled-coil structures, we gain the traces shown in Figure 2a–c with increased signal-to-noise ratio. For LZ10 coiled coils without any added unstructured subsegments, mechanical unfolding (black trace in Figure 2a) starts at forces of 12 pN whereas refolding (blue trace) occurs around 7.8 pN.^[19] For the coiled coils with added unstructured amino acids, the average unzipping force trace (black in Figure 2b for LZ10₊₁₀ and black in Figure 2c for LZ10₊₂₀) remains unchanged within the experimental error. This shows that insertion of additional amino acids within the C-terminal end of the nucleation seed does not alter the unfolding process.

In contrast, the averaged folding-force trace strongly depends on the number of added unstructured amino acids (blue traces in Figure 2b and 2c). With increasing size of the added, unstructured subsegment, the average refolding force decreases, thereby leading to a higher hysteresis between unzipping and reziping traces (yellow area in Figures 2a–c). To reproduce the experimentally measured force traces theoretically, we performed a kinetic Monte Carlo simulation based on

the two-state energy landscape shown in Figure 2e. This Monte Carlo simulation is explained in the Experimental Section. In brief, the coiled coil can either populate the totally folded state (green dot at 0 opened turns in Figure 2e) or the totally opened state (green dots at 21 $k_B T$ for the respective coiled coils). The barrier separating both states (green square in Figure 2e) defines the rates with which the system switches between the closed and open states. The height of the barrier depends in a nonlinear fashion on the applied mechanical force, where the simulation also accounts for the elastic contributions of stretching the whole protein construct. Increasing the applied force decreases the height of the unfolding barrier, while the refolding barrier height increases. The energy landscape for the unmodified LZ10 coiled coil was already mapped in earlier measurements^[20,21] and therefore the absolute position of the transition state (TS) is well determined (green square in Figure 2e). Thus, the size of the nucleation seed for the unchanged LZ10 model coiled coil results in 4 ± 1 turns (red landscape in Figure 2e). The Monte Carlo simulation fully reproduces the measured force traces of the different coiled coils (red in Figures 2a–c) with the energy landscapes shown in Figure 2e in red, blue and black, respectively. The only parameter that was adjusted to model refolding of the three different coiled coils was the length of the unfolded polypeptide chain due to the amino-acid inserts. Therefore, the C-terminal addition of unstructured subsegments only increases the size of the nucleation seed without having any influence on the absolute position of the transition state (green square in Figure 2e) or the total free energy of unfolding (green dots at $21 \pm 2 k_B T$ in Figure 2e).

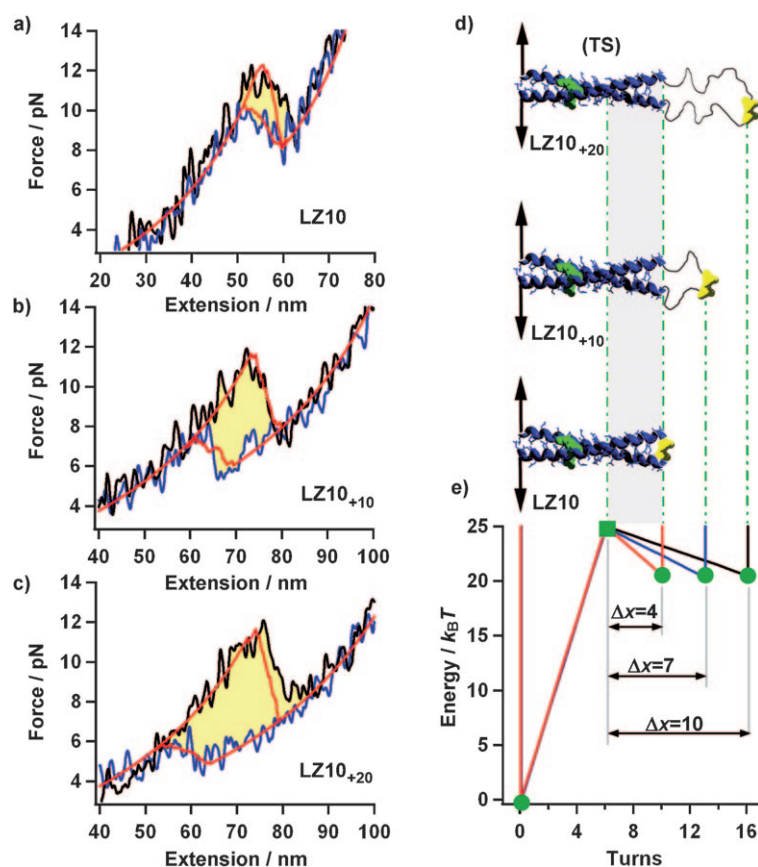


Figure 2. Effect of the nucleation seed size on the averaged unfolding and folding properties of a model coiled coil. a) Averaged unfolding (black) and refolding (blue) force trace of the unmodified LZ10 model coiled coil measured at pulling velocities of 750 nm s^{-1} , adapted from ref. [21]. b) Averaged unfolding (black) and refolding (blue) traces of the LZ10 coiled coil with C-terminal addition of ten amino acids, measured at velocities of 500 nm s^{-1} . c) Averaged unfolding (black) and refolding (blue) traces of the LZ10 coiled coil with addition of 20 unstructured amino acids, measured at velocities of 500 nm s^{-1} . The red traces (a)–(c) are calculated by means of Monte Carlo simulations. d) Schematic structures of the designed coiled coils. e) Energy landscapes used for the Monte Carlo simulations.

In turn, the fact that the total energy of unfolding does not change with the addition of unstructured subsegments corroborates the view that this part of the hinge region from the *D. melanogaster* kinesin is indeed unstructured. This finding is also in good agreement with ensemble studies on the human kinesin neck-coiled coil, where it was shown that the addition of the hinge only has minor effects on the total free energy of unfolding.^[26]

In our coiled-coil constructs, the size of the nucleation seed (i.e. the contour length of the polypeptide chain that forms the nucleation seed) is linearly connected to the amount of added unstructured amino acids (see Figure 2e). This allows us to directly probe the dependency of the average refolding force on the width of the refolding barrier Δx . Figure 3 shows

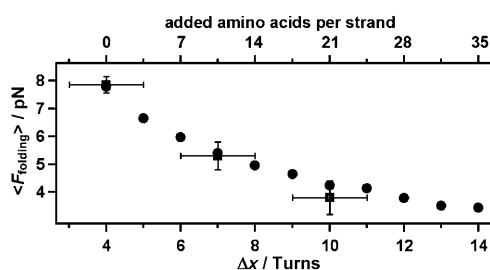


Figure 3. Average folding force in dependence of the nucleation seed size. The squares (■) are the experimental values measured at an average velocity of 700 nm s^{-1} . Bars denote the standard error of the mean. Circles (●) are averaged folding forces calculated from the Monte Carlo simulation based on the energy landscapes shown in Figure 2e.

the measured average refolding forces for the coiled coils with added unstructured subsegments as squares. Mean refolding forces of about six force traces, such as the ones shown in Figures 2a–c, were averaged leading to ≈ 360 evaluated single force traces for the respective values in Figure 3. The mean refolding force decreased from 7.8 pN for the unmodified LZ10 coiled coil to 5.4 and 3.7 pN when the nucleation seed size was increased by 10 and 20 unstructured amino acids per strand, respectively. To model the force dependence of refolding, the change of barrier heights with force needs to be calculated. However, the barrier height depends on the applied force in a nonlinear fashion, and the commonly used approximation of a barrier height depending linearly on the applied force ($\Delta G^\ddagger(F) = F\Delta x^\ddagger$) does not hold. Other theoretical models are available that can be used to describe the refolding process of proteins.^[27–29] The circles in Figure 3 correspond to the mean refolding forces calculated as function of the nucleation seed contour length obtained by the Monte Carlo simulation, as described in [20]. The simulation accounts for the elastic contributions needed to stretch the polypeptide to a certain extension using the worm-like-chain (WLC) model.^[30] Apparently, the energetic contribution for the contraction of the elongated unfolded nucleation seed against a force is a main determinant of the folding process. This mechanism also controls folding of globular proteins against force, where a similar behavior was recently observed experimentally.^[31]

Conclusions

In summary, our experiments show that the addition of unstructured subsegments onto a coiled coil leads to an increase in the size of the nucleation seed which in turn causes a direct decrease of the refolding forces of the coiled coil. This means that the homogenous segments of naturally occurring coiled coils, which are often interrupted by unstructured subsegments, can be seen as local subunits which have to form their own nucleation seed. The size of such a nucleation seed would then consist of the intrinsic nucleation seed of the subunit plus the following unstructured subsegment. Our findings now allow the design of coiled coils with refolding forces ranging between 0 and 7.8 pN by simply adding unstructured amino acids. A possible application could lie in the construction of tunable force sensors, which are able to discriminate physiological relevant forces in the lower pN regime.

Experimental Section

To mechanically unzip the coiled coils LZ10, LZ10_{+10r}, and LZ10_{+20r} we fused globular protein domains from the *Dyctostelium discoideum* filamin (ddFLN 1–5) to the N-terminal end of the respective structures. This led to protein constructs similar to that shown schematically in Figure 4c for the LZ10₊₂₀ coiled coil. The amino acid sequences of the coiled-coil constructs are given in Figure 4a.

When measured with AFM, one strand of the protein dimer can bind unspecifically to the AFM cantilever tip while the other strand can bind to the substratum. All measurements were conducted with a custom-built AFM equipment at room temperature in phosphate buffered saline (PBS) solution using type-B bio-levers from Olympus (Tokyo). Retraction of the cantilever from the substratum led to unzipping of the coiled coil at forces below 20 pN (see Figure 4b), followed by the unfolding of individual ddFLN 1–5 protein domains around 60 pN. This unfolding pattern allows selection of true single-molecule force traces attached in the desired unzipping geometry. All measured traces on a single molecule that exhibit two ddFLN4 unfoldings also showed coiled-coil unfolding events in the low-force regime. To increase the signal-to-noise ratio in this low-force regime, we consecutively recorded and averaged approximately 12 unzipping (black in Figure 4b) and rezipping (blue in Figure 4b) cycles on the same molecule. For the averaging procedure we included all collected backward traces; for the forward cycles we only excluded the rarely occurring traces where no prior refolding was observed. Averaging the pre-averaged traces together with those from about five different measurements on the same construct led to the force trace shown in Figure 4d (see also Figures 2a–c). Only comparable measurements were averaged, that is, only those that showed the same amount of pre-unfolded ddFLN domains and were conducted at the same velocity. The averaging procedure led to a signal-to-noise ratio that was increased by a factor of seven. The average unzipping force trace (black in Figure 4d) followed—up to 12 pN—the WLC force-extension behavior^[30] of the folded state [1], and after unfolding, the WLC trace of the unfolded state [2]. The averaged refolding trace (blue) skips between extensions A and B from the unfolded state (WLC trace [2]) to the folded state (WLC trace [1]). Therefore, the most probable refolding force lies at $4.1 \pm 0.8 \text{ pN}$ (grey area in Figure 4c) for the shown force trace. The average of about six of such values of the most probable refolding force leads to the data points shown

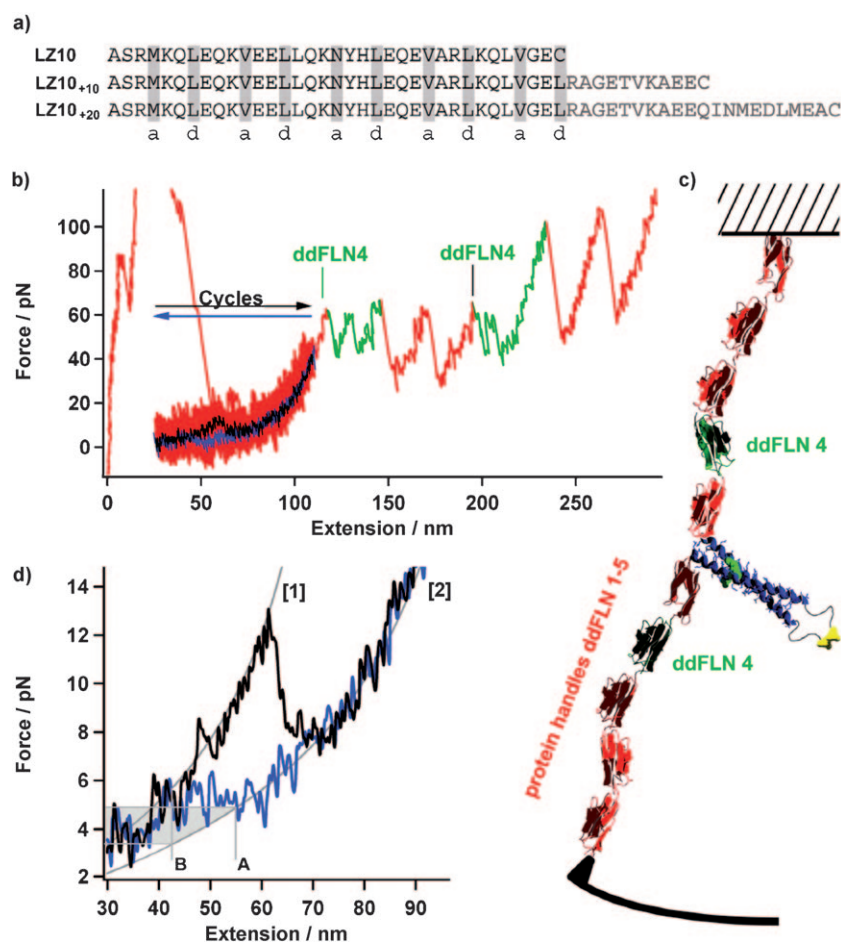


Figure 4. Experimental setup for the mechanical unzipping of coiled coils: a) Amino-acid sequences of the measured coiled-coil constructs. The heptad sequence is given for the LZ10 coiled coil, the added unstructured amino acids are given in grey. b) Typical force curve of the protein construct. Around 60 pN unfolding of the protein handles occurs, while coiled-coil unzipping takes place at forces < 20 pN. The averaged coiled-coil unzipping and re-zipping force traces from this regime are shown in black and blue, respectively. c) Schematic structure of the measured protein construct. The protein handles are added N-terminally to the respective coiled coils to allow attachment of cantilever tip and surface to the protein in the desired unzipping geometry. d) Average of comparable coiled-coil unzipping (black) and re-zipping (blue) force traces from about five different, pre-averaged traces, such as those in (b).

in Figure 3, which comprise a total of about 360 single force traces.

For the Monte Carlo simulation, we defined an energy landscape as a function of open turns, as shown in Figure 2e, where the coiled coil can populate either the folded state or the unfolded one. To switch between the states, the coiled coil has to overcome the transition state (TS), which is schematically shown in Figure 1 for the unchanged LZ10 construct and is defined by the height and position of the energetic barrier that separates the folded and unfolded states. The force-dependent barrier height defines (via an Arrhenius-like equation) the rates of unfolding and refolding. By retracting the virtual cantilever from the surface, a force is applied to the N-terminal end of the coiled coil. This tilts the energy landscape where the elastic contributions needed to stretch the unfolded polypeptide are included. A detailed description for the calculation of the tilted energy landscape is given in ref. [20]. The occurrence of a transition between the unfolded and folded states is determined by a random variable. We calculated 30 different forward and backward traces and averaged them with the same procedure used to average the experimental data.

Acknowledgements

We thank Erich Sackmann for his stimulating ideas and wish him a happy birthday. We thank Günther Woehlke, Manfred Schliwa, and Johannes Stigler for stimulating discussions. Financial support of the German Excellence Initiative, via the Nanosystems Initiative Munich and the Deutsche Forschungsgemeinschaft SFB 486, is gratefully acknowledged.

Keywords: atomic force microscopy · coiled-coil design · GCN4 · mechanical unzipping · protein folding

- [1] A. N. Lupas, M. Gruber, *Adv. Protein Chem.* **2005**, *70*, 37–78.
- [2] J. M. Mason, K. M. Arndt, *ChemBioChem* **2004**, *5*, 170–176.
- [3] D. A. Parry, R. D. Fraser, J. M. Squire, *J. Struct. Biol.* **2008**, *163*, 258–269.
- [4] R. Simson, E. Wallraff, J. Faix, J. Niewohner, G. Gerisch, E. Sackmann, *Biophys. J.* **1998**, *74*, 514–522.
- [5] H. Herrmann, H. Bar, L. Kreplak, S. V. Strelkov, U. Aebi, *Nat. Rev. Mol. Cell Biol.* **2007**, *8*, 562–573.
- [6] S. J. Everse, G. Spraggon, L. Veerapandian, M. Riley, R. F. Doolittle, *Biochemistry* **1998**, *37*, 8637–8642.
- [7] J. Rizo, C. Rosenmund, *Nat. Struct. Mol. Biol.* **2008**, *15*, 665–674.
- [8] W. Weissenhorn, A. Dessen, L. J. Calder, S. C. Harrison, J. J. Skehel, D. C. Wiley, *Mol. Membr. Biol.* **1999**, *16*, 3–9.
- [9] E. Wolf, P. S. Kim, B. Berger, *Protein Sci.* **1997**, *6*, 1179–1189.
- [10] E. M. Dagenbach, S. A. Endow, *J. Cell Sci.* **2004**, *117*, 3–7.
- [11] T. Hodge, M. J. Cope, *J. Cell Sci.* **2000**, *113*, 3353–3354.
- [12] J. Harborth, K. Weber, M. Osborn, *EMBO J.* **1995**, *14*, 2447–2460.
- [13] M. Chana, B. P. Tripet, C. T. Mant, R. S. Hodges, *J. Struct. Biol.* **2002**, *137*, 206–219.
- [14] E. K. O'Shea, J. D. Klemm, P. S. Kim, T. Alber, *Science* **1991**, *254*, 539–544.
- [15] L. B. Moran, J. P. Schneider, A. Kentsis, G. A. Reddy, T. R. Sosnick, *Proc. Natl. Acad. Sci. USA* **1999**, *96*, 10699–10704.
- [16] W. K. Meisner, T. R. Sosnick, *Proc. Natl. Acad. Sci. USA* **2004**, *101*, 13478–13482.
- [17] K. J. Lumb, C. M. Carr, P. S. Kim, *Biochemistry* **1994**, *33*, 7361–7367.
- [18] J. A. Zitzewitz, B. Ibarra-Molero, D. R. Fishel, K. L. Terry, C. R. Matthews, *J. Mol. Biol.* **2000**, *296*, 1105–1116.
- [19] T. Bornschlöggl, M. Rief, *Phys. Rev. Lett.* **2006**, *96*, 118102.
- [20] T. Bornschlöggl, M. Rief, *Langmuir* **2008**, *24*, 1338–1342.
- [21] T. Bornschlöggl, G. Woehlke, M. Rief, *Proc. Natl. Acad. Sci. USA* **2009**, *106*, 6992–6997.
- [22] C. Seeberger, E. Mandelkow, B. Meyer, *Biochemistry* **2000**, *39*, 12558–12567.
- [23] A. H. Crevenna, S. Madathil, D. N. Cohen, M. Wagenbach, K. Fahmy, J. Howard, *Biophys. J.* **2008**, *95*, 5216–5227.

- [24] B. Tripet, R. D. Vale, R. S. Hodges, *J. Biol. Chem.* **1997**, *272*, 8946–8956.
- [25] M. Thormahlen, A. Marx, S. Sack, E. Mandelkow, *J. Struct. Biol.* **1998**, *122*, 30–41.
- [26] B. Tripet, R. S. Hodges, *J. Struct. Biol.* **2002**, *137*, 220–235.
- [27] E. Evans, K. Ritchie, *Biophys. J.* **1997**, *72*, 1541–1555.
- [28] R. B. Best, G. Hummer, *J. Am. Chem. Soc.* **2008**, *130*, 3706–3707.
- [29] M. Schlierf, F. Berkemeier, M. Rief, *Biophys. J.* **2007**, *93*, 3989–3998.
- [30] C. Bustamante, J. F. Marko, E. D. Siggia, S. Smith, *Science* **1994**, *265*, 1599–1600.
- [31] M. Schlierf, M. Rief, *Angew. Chem.* **2009**, *121*, 835–837; *Angew. Chem. Int. Ed.* **2009**, *48*, 820–822.

Received: July 20, 2009

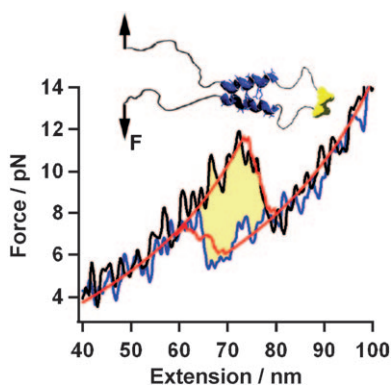
Published online on ■ ■ ■, 2009

ARTICLES

T. Bornschlög, * J. C. M. Gebhardt, M. Rief



Designing the Folding Mechanics of Coiled Coils



Coiled-coil folding: By controlling the size of the nucleation seed the authors are able to adjust the mean refolding force of a model coiled coil in the range between 0 and 8 pN (see picture).